

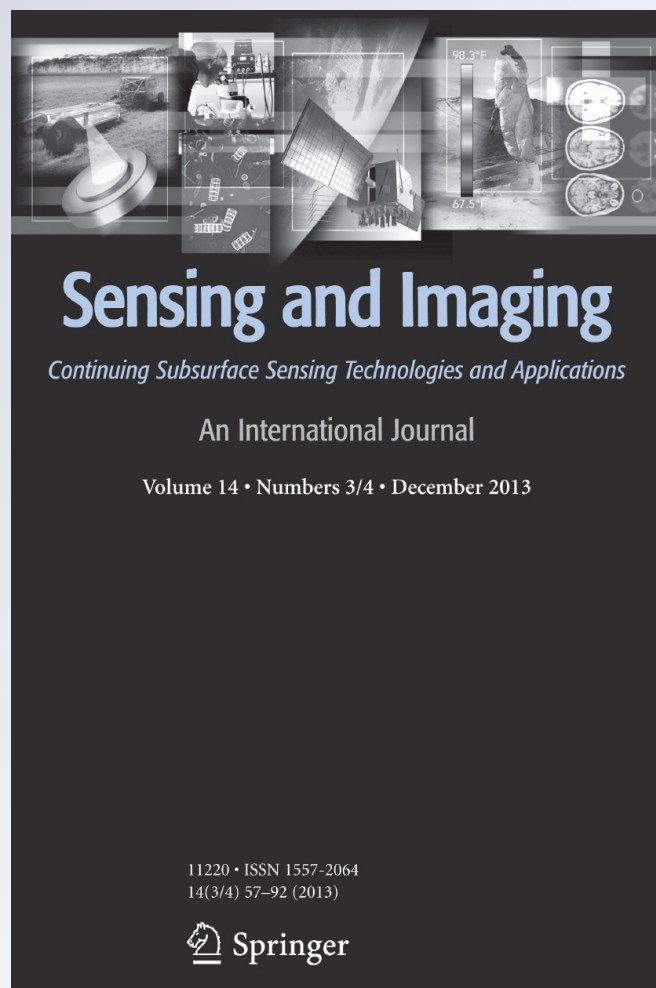
Eddy Current Sensing of Torque in Rotating Shafts

Orestes J. Varonis & Nathan Ida

Sensing and Imaging: An International Journal
Continuing Subsurface Sensing Technologies and Applications

ISSN 1557-2064
Volume 14
Combined 3-4

Sens Imaging (2013) 14:81-92
DOI 10.1007/s11220-013-0080-6



Your article is protected by copyright and all rights are held exclusively by Springer Science +Business Media New York. This e-offprint is for personal use only and shall not be self-archived in electronic repositories. If you wish to self-archive your article, please use the accepted manuscript version for posting on your own website. You may further deposit the accepted manuscript version in any repository, provided it is only made publicly available 12 months after official publication or later and provided acknowledgement is given to the original source of publication and a link is inserted to the published article on Springer's website. The link must be accompanied by the following text: "The final publication is available at link.springer.com".

Eddy Current Sensing of Torque in Rotating Shafts

Orestes J. Varonis · Nathan Ida

Received: 15 January 2013 / Revised: 8 September 2013 / Published online: 10 October 2013
© Springer Science+Business Media New York 2013

Abstract The noncontact torque sensing in machine shafts is addressed based on the stress induced in a press-fitted magnetoelastic sleeve on the shaft and eddy current sensing of the changes of electrical conductivity and magnetic permeability due to the presence of stress. The eddy current probe uses dual drive, dual sensing coils whose purpose is increased sensitivity to torque and decreased sensitivity to variations in distance between probe and shaft (liftoff). A mechanism of keeping the distance constant is also employed. Both the probe and the magnetoelastic sleeve are evaluated for performance using a standard eddy current instrument. An eddy current instrument is also used to drive the coils and analyze the torque data. The method and sensor described are general and adaptable to a variety of applications. The sensor is suitable for static and rotating shafts, is independent of shaft diameter and operational over a large range of torques. The torque sensor uses a differential eddy current measurement resulting in cancellation of common mode effects including temperature and vibrations.

Keywords Torque sensors · Eddy current measurements · Magnetoelastic materials

1 Introduction

Torque sensing has received considerable attention with a variety of methods and sensors available commercially. In general, torque sensing requires two separate

O. J. Varonis
Advanced Control Systems, The Timken Company, Canton, OH 44706-0930, USA
e-mail: orestes.varonis@timken.com

N. Ida (✉)
Department of Electrical and Computer Engineering, The University of Akron, Akron,
OH 44325-3904, USA
e-mail: ida@uakron.edu

functions. The first of these is the induction of stress due to torque either in a separate component or in a component of the device in which torque is sensed, such as the shaft of a machine. The second function is the sensor proper, capable of quantifying the stress or its effects. The two functions may be accomplished in any number of methods many of which have been implemented and described. One of the simplest methods of generating torque-induced stress is to use a thin metal shaft and use the shear strain on its outer surface as a measure of torque [1]. In ferromagnetic shafts, the effect of stress on electric conductivity and magnetic permeability can be used directly, with the measurement taking place on the surface of the shaft. The sensitivity can be improved by special means such as the introduction of shallow grooves around the circumference of the shaft, properly aligned with the direction of the principal lines of stress. In addition, because the properties vary around the circumference, the electric conductivity and magnetic permeability measurements are averaged over a rotation [2]. Another method is to use two magnetostrictive sleeves, circularly magnetized in opposite direction and to sense the magnetization vector which, of course, is a function of permeability and hence of stress [3]. Alternatively, one can use these sleeves without the magnetization and sense the change in conductivity or permeability [4]. In nonmagnetic shafts one can use two thin strips of magnetostrictive films, aligned with the direction of maximum strain and sense the change in conductivity as above [5]. There are many other variants of the methods described above [6, 7]. In all these methods, one relies on the fact that strain/stress introduced by the torsion of the shaft or an attached member causes changes in conductivity and permeability. The stress may be induced in the shaft itself, in auxiliary members [1, 2] or as in the case described here, in a magnetoelastic sleeve integral with the shaft.

The most common method of sensing of torque is through use of strain gauges, optical, magnetic or eddy current sensors [3, 6, 7].

The use of strain gauges is almost obvious since in all cases one measures the strain produced by torque or an equivalent quantity. In applications with strain gauges, these are attached directly to the strained member in the directions of maximum strain ($\pm 45^\circ$ to the main axis of a shaft, for example) [1]. Typically the gauges are connected in a bridge configuration to compensate for temperature and other common source noises such as vibrations. However, for shaft applications, the signals must be transmitted through a rotational transformer, complicating the sensor considerably [1]. Both power and bridge output must be transferred across this transformer. In optical systems, a typical configuration is that of slotted disks at two different locations on the shaft and the displacement of slots due to torsional differences are related to torque [4]. Similar effects can be achieved with alternating white/black painted strips and use of reflection rather than transmission of light. Although optical systems of sensing are attractive in their simplicity and noise figures, they are affected by dust and dirt, a serious problem in the industrial environment.

Magnetic sensing of torque has received considerable attention and there are a number of configurations that have been used. One, mentioned above makes use of two magnetoelastic sleeves, circularly magnetized, fixed to the shaft [3]. Hall elements are placed next to the sleeves at two positions, 180° apart. In the absence

of torque, the outputs of the Hall elements are zero. When torque is applied, the magnetization of the sleeves becomes elliptical and the output of the two sensors changes. The difference between the two is a measure of torque. The differential output also helps with temperature drift and noise in the sensors. Another form of sensing makes use of a single magnetoelastic sleeve and a differential transformer whose flux closes through the sleeve. A primary coil generates the flux and two differentially connected coils serve as the sensors. Normally the output is zero as the sleeve's permeability is constant and the induced emf in the two coils is the same. In the presence of torque, the stressed sleeve will have different permeabilities at different locations. The position of the coils is such that the flux closes through different paths for each of them and hence each will produce a different induced voltage [2]. Magnetic reluctance has also been used for torque measurements. The basic idea is that the torsion of a member can move two separate magnetic pieces closer together (or further apart) as the torque increases. The reluctance can then be a measure of torque. A particular configuration [5], employs two toothed rings so that under no torque the teeth are centered and the gaps between them is constant and uniform. The two rings are fixed at two different locations axially so that torque on the shaft will change the reluctance. Two coils are used so that the difference between their emfs is zero (or nearly zero) in the absence of torque, the emf then increases with the applied torque.

The most common method of torque sensing using eddy currents employs two encircling coils, and a pair of thin nonmagnetic, slotted sleeves with slots on top of each other and aligned under no torque conditions. The sleeves, serve to attenuate the magnetic field with attenuation at minimum when the sleeves are aligned (no torque). As the shaft is torqued, the slots move with respect to each other increasing losses (attenuation). The attenuation of the field is proportional to torque and hence the differential impedance of the eddy current coils is a direct indication of torque [1]. In these methods the coils encircle the shaft so that they are stationary and require no particular mechanical considerations. Another possibility of eddy current sensing is based on the fact that the permeability and conductivity of the shaft, or of a fitted magnetostrictive ring change around the circumference. A number of eddy current coils are disposed around the circumference serving as simple proximity sensors, driven at a fixed frequency. The impedance of the coils is monitored and from the distribution around the shaft one can infer the torque [7].

The method described here uses a press-fitted C250 Maraging Steel (18 % Ni, 8.5 % Co, 5 % Mo, 0.4 % Ti, 0.1 % Al) sleeve tightly fit over the shaft. Torqueing the shaft transfers stress to the sleeve and that generates tension and compression at 90° to each other in the sleeve (see Fig. 1a). Two stationary, non-contacting eddy current probes are placed against the sleeve at 90° to each other so that one coil senses the metal under compression, the other under tension. Since the steel used exhibits positive Villari effect, the local permeability increases for sections under tension and decreases for sections under compression (Fig. 1b). This then changes the induced eddy currents for the two coils and hence the induced emf in the coils. Since the coils are in differential mode, the emf measured across the sensor increases with torque with zero output for no torque.

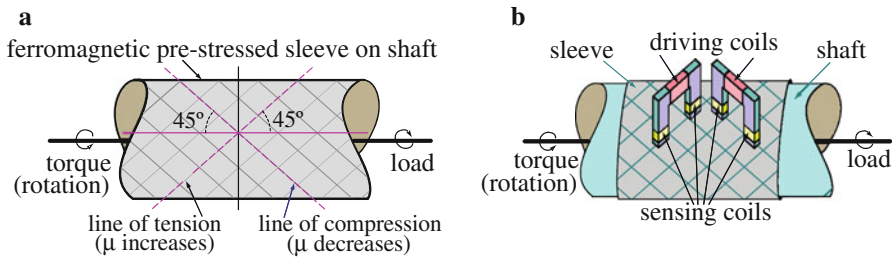


Fig. 1 The proposed method of torque sensing. **a** Lines of tension and compression on the magnetoelastic sleeve due to torque. **b** Orientation of the two eddy current probes to sense the changes in permeability. The sensing coils in each probe are connected in series opposing (differential sensor)

The development of the measuring system consists of a number of steps, each important for the final result and performance of the system. The first is the eddy current evaluation of the maraging steel sleeve since its performance is critical to the overall performance of the sensing system. The eddy current coils, configured in a differential probe have received particular attention and will be described below in some detail. Particular attention was given to repeatability of results and hence to the problem of lift-off of the eddy current probes with respect to the rotating sleeve since any variation in distance between probe and sleeve causes variations in output and hence errors in reading of torque. In conjunction with the above, a commercial eddy current instrument is used to drive the coils, pick up the induced emf and analyze the output. This frees the system from systemic errors due to associated electronics and, in addition, the instrument is used for evaluation of the probe and the maraging steel sleeve.

2 An Exploratory Eddy Current Probe

The purpose of this preliminary evaluation is two-fold. The first, and most important is to ascertain working parameters for the sensor. This includes operating frequency, field levels and acceptable liftoff of the probe. Second, the tests give indication on sensitivity expected and errors to be treated. The tests were done by application of static torque on a specially constructed test rig and with the use of a commercial eddy current instrument. Additional aspects of the evaluation are those of the eddy current instrument itself, DC offset of the signals and effect of harmonics on performance. The frequency response evaluation includes two important characteristics. One attempts to identify the “best” frequency for the sensor taking into account the fact that the real and imaginary components of the probe response (referred here as the x and y components) have different characteristics with frequency. The second part of the evaluation attempts to identify the effects of liftoff and DC offset on the output signal with the purpose of attaining maximum sensitivity. To perform the tests, an exploratory probe, shown in Figs. 2 and 3 was developed. The probe includes a driving coil in the center of the probe and two

pickup coils shown on the tips of the probe. In actual implementation (Fig. 3a), both the driving coil and each of the pickup coils are split in two. Figure 2b shows the driving and pickup coil connections to the eddy current instrument showing how the split driving coils is driven and how the pickup coils are connected to amplifiers and signal conditioning stages. The excitation coil consists of 36 turns capable of a maximum current of 1.4 A rms. The pickup coils each consists of 150 turns and are placed close to the tip of the probe. The core of the probe is laminated, and the assembly is epoxy potted to obtain a practical device for testing, shown in Fig. 3b. Each pole of the probe is 3 mm by 1.5 mm in cross-section, width of 11 mm and length of probe is 24 mm. Core material is SuperPerm-49 [8]. Its composition consists of 0.02 % C, 0.50 % Mn, 0.35 % Si, 48.00 % Ni, and 51.13 % Fe. The material has been designed to be used in laminated cores for instrument transformers, magnetic shields, and applications that require high permeability values at low magnetizing force.

The final relevant properties of the probe are shown in Table 1.

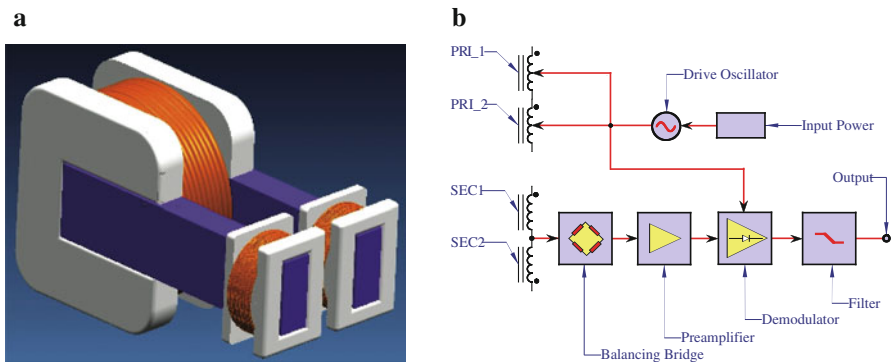


Fig. 2 **a** Principle of the eddy current coil showing the driving coil and the two sensing coils. **b** The driving and sensing block diagram. Note the split driving coil and the orientation of the emfs in the driving and sensing coils

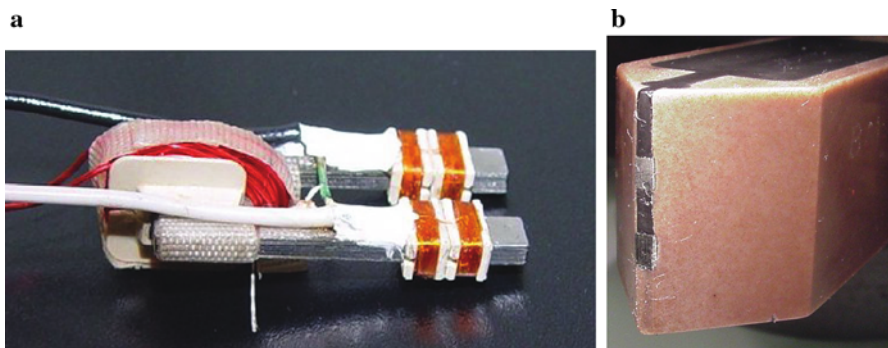


Fig. 3 **a** The wound eddy current probe showing the laminations, the driving coil and the two sensing coils, each split in two. **b** Detail of the completed, potted and shaped probe. The tips of the core can be seen as the lowest and third rectangle from the bottom

Table 1 Electric properties of the exploratory probe

	Excitation winding	Sensing windings
Resistance	0.417 Ω	15.32 Ω
Inductance in air	86.3 μH	5.4 mH
Inductance with core tips against maraging steel sleeve	119 μH	6.6 mH

3 C-250 Maraging Steel Eddy Current Evaluation

The evaluation of the maraging steel sleeve starts with the appropriate frequency for testing. The range of frequencies, from 2 Hz to 128 kHz is used. To do so a range of torque values is applied and the eddy current probe response recorded. The probe was placed at various angles to the shaft but only representative results with the probes aligned along the compression and tension lines (45° and 135°) are shown here. In the evaluation, an attempt was made to find a single operating frequency that optimizes the output and hence optimizes the sensitivity of the sensor overall. This is important since the coil has both real and imaginary components and they cannot be maximized independently and their maxima occur at different frequencies. Figure 4 shows the maximum normalized coil emf variation with respect to frequency (real, imaginary and magnitude) at a fixed liftoff of the coil. The real part of the emf peaks at about 16 kHz but the imaginary part decreases with frequency, a typical effect in eddy current testing. Normalization in this case means the impedance is normalized with respect to coil reactance with the coil in air, at the test frequency. Figure 5 shows the probe response with respect to torque at 4 kHz and at 16 kHz, again showing the real, imaginary and absolute normalized values. Figure 6 shows the response at 1 kHz. The sensitivity is maximum at 1 kHz followed by that at 4 kHz and then at 16 kHz. These results were evaluated for other angles, more specifically at 45° but also at 0° and 90° . Lower and higher frequencies provide reduced sensitivities. However, these frequencies are probe-specific and relate to the inductance of the coils. Any modifications to the probe will change its performance and sensitivity. Although the signal shown in Fig. 6 seems to be less linear than those at 4 and 16 kHz, that is not the case at all angles. The sensitivity was deemed most important, hence the selection of 1 kHz as the operating frequency. In addition, multiple measurements show a spread in the signal obtained. For this reason, the signal is further processed using either a linear best fit or a polynomial fit to obtain the response of the probe (see Sect. 4 on results).

Another probe characteristic that required careful evaluation was the effect of liftoff on probe response and, more importantly, on the torque reading. To do so, the response was measured at various frequencies. The effect increases with decrease in frequency as can be seen in Fig. 7. Clearly, the change in emf due to liftoff can be interpreted as being due to torque and vice versa. This means that it is critical that liftoff be eliminated or at the very least, tightly controlled especially at the lower frequencies. Since the sensitivity is higher at lower frequencies the problem of liftoff control is an integral part of the development of the present sensor.

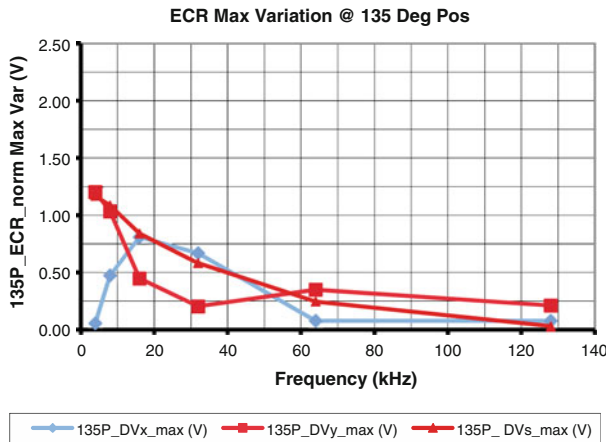


Fig. 4 Eddy current probe response with frequency showing the real part (135P_DVx_max curve), imaginary part (135P_DVy_max curve) and the magnitude of the emf (135P_DVs_max curve)

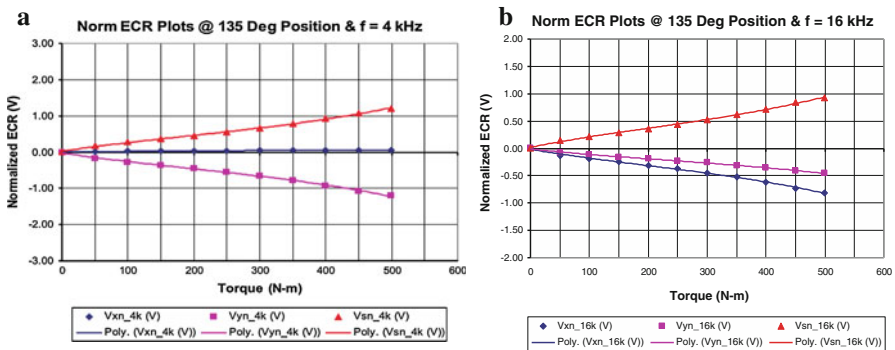


Fig. 5 Eddy current probe response with torque at 4 and 16 kHz. The *solid lines* are the polynomial fit to the measured data. Vxn represents the real par, Vyn the imaginary part and Vsn the magnitude, all normalized

Based on the exploratory probe and its performance and the need for a constant gap measurement a single probe, containing two coils arranged at 90° to each other was designed and re-evaluated. One probe is shown in Fig. 8a. The driving coil, split in two, contains 40 turns (see Table 2) and the sensing coil contain each 150 turns. The driving coil has been moved closer to the sensing coils to reduce the total length of the probe. The core is similar to that of the exploratory coil but it is slightly thicker and the poles separated further apart. These changes reduce the inductance of the probe and, as a result the probe's maximum sensitivity is higher, around 10 kHz. The electric properties are shown in Table 2. Two of these probes are housed together, aligned 90° to each other (the housing is shown in Fig. 8b) so that one probe senses along the compression lines whereas the second on the tension lines. The complete probe, potted and connected to a connector is shown in Fig. 8c. The probe iron-probe tips can be seen on the probe surface at bottom right of the

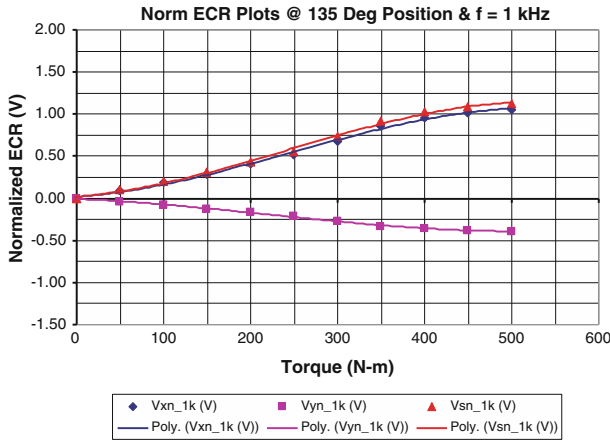


Fig. 6 Eddy current probe response against torque at 1 kHz showing highest sensitivity. The frequency was selected as the basic frequency for the sensor

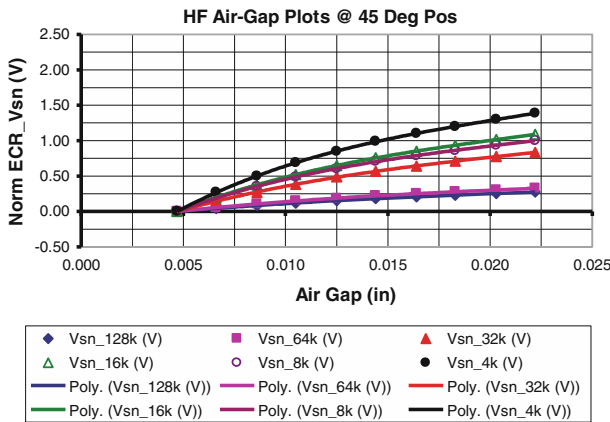


Fig. 7 Effect of lift-off on the eddy current probe response at various frequencies. The solid lines connecting the measurement points were obtained by polynomial fit

figure. As mentioned above, a particular concern in the design was the air gap between the probe and the maraging steel ring. To solve this problem, the probe was incorporated into a circular housing that incorporates two bearings, one on each side of the sleeve so that the probe is stationary while the sleeve rotates with the shaft. The air gap remains constant within the tolerances of the bearings. The probe assembly on the shaft is shown in Fig. 8d.

In effect, each eddy current coil (consisting of a driver and two pickup coils as in Fig. 8a) is a variable reluctance transformer whereby the change in reluctance is due to torque. The variable reluctance in this case is provided by the change in permeability due to torque. The measurement method is shown in Fig. 2b where the connections of the coil and the basic elements of the sensor are shown. The bridge

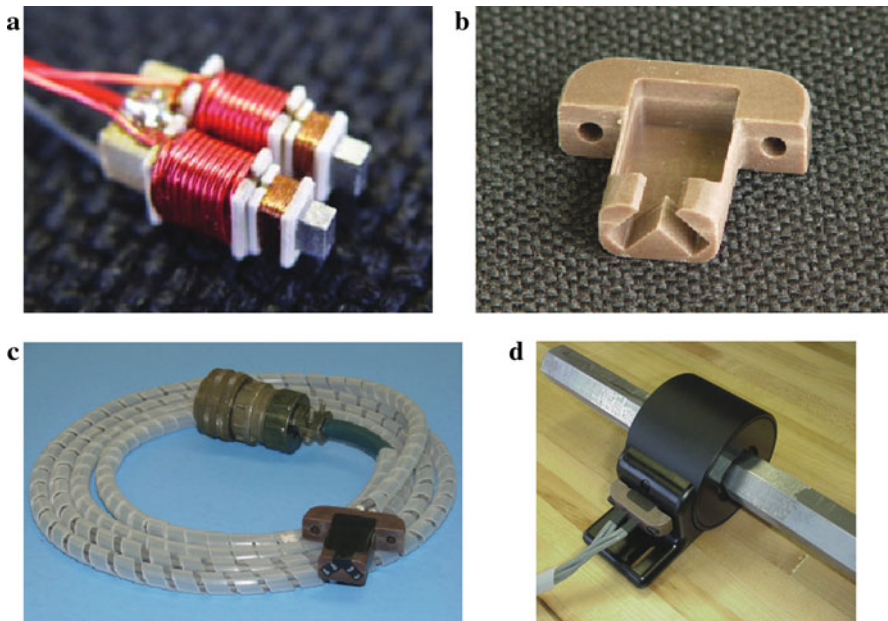


Fig. 8 **a** The modified probe with split driving coils and split sensing coils. **b** The probe housing, ready to accept two probes, oriented 90° to each other. **c** Complete probe after potting and connection to an eddy current instrument connector. **d** Complete probe housed in the constant gap housing on a shaft

Table 2 Properties of the constant-gap dual sensor probe

	Excitation winding	Sensing windings
Number of turns	40	300 (150 on each pole)
Wire gauge	26 AWG (0.321 mm)	44 AWG (0.0508 mm)
Resistance	3.47 Ω	40 Ω
Inductance with core tips against maraging steel sleeve	92.6 μ H	3.62 mH

connection eliminates the induced voltage on the coils due to the driving coils in the absence a sensing quantity whereas the demodulator and the filter convert the emf into a dc level. The outputs of the two probes are summed internally in the eddy current instrument to produce an emf proportional to torque.

4 Results

The sensor can be driven at various frequencies but the most suitable frequency was found to be around 10 kHz, based on the probe response and skin depth. To evaluate

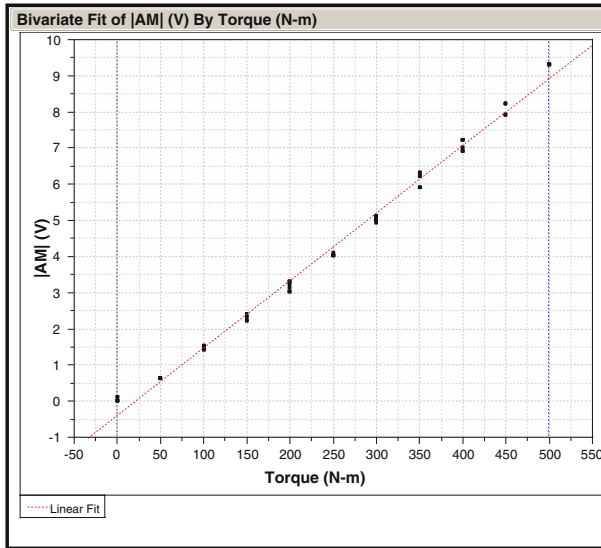


Fig. 9 Voltage amplitude (|AM|) versus torque: raw output and linear best-fit transfer function (200 rpm). Error is 0.139 % FS

the appropriate frequency, the measured output was correlated with the torque and the response with the best correlation was selected since it represents the least spread in measured values. Nevertheless, the frequency is not critical and the present probe can operate successfully from about 1 to 20 kHz with minor changes in performance. Figure 9 shows the raw output together with a linear best fit for torque varying between 0 and 900 N.m. The linear best fit represents a maximum error of 0.139 % FS or a maximum measurement error of ± 0.697 N.m (compared to measured data). The linear best fit produced a correlation with $R^2 = 0.994$. The linear best-fit curve is:

$$V = -0.386337 + 0.0186461T \quad [\text{V}]$$

where T is the torque in [N.m].

The sensitivity of the sensor therefore is 18.646 mV/(N.m).

The transfer function in Fig. 9 is slightly nonlinear and therefore a polynomial fit is more appropriate, especially if higher accuracy is required. Figure 10 shows the same result with a 3rd order polynomial fit. The transfer function is:

$$V = -0.688339 + 0.0189343T + 9.2 \times 10^{-9}(T - 249.868)^2 - 6.4836 \times 10^{-9}(T - 249.868)^3 \quad [\text{V}]$$

The sensitivity can be calculated directly as:

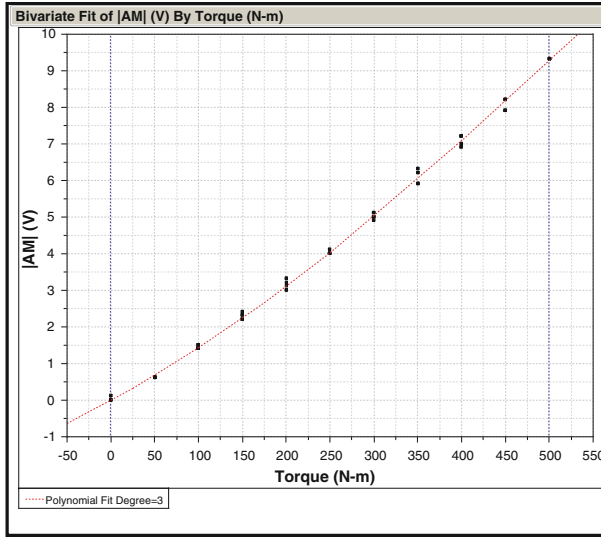


Fig. 10 Voltage amplitude versus torque: raw output and 3rd order polynomial fit transfer function (200 rpm). Error is 0.065 % FS

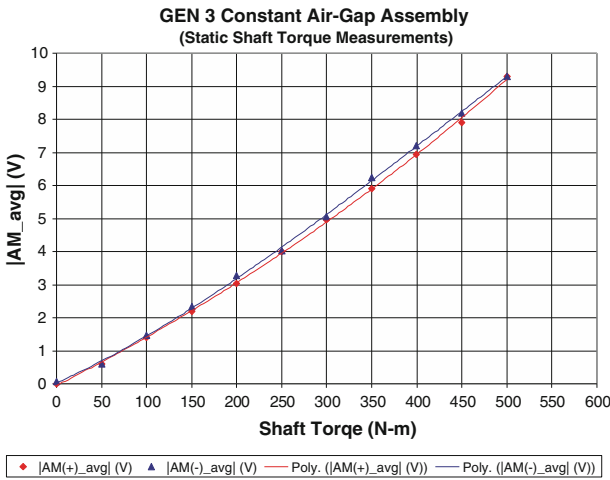


Fig. 11 Hysteresis errors. Maximum error is approximately 0.016 % FS

$$s = \frac{dV}{dT} = 0.0189343 + 9.2 \times 10^{-9}(T - 249.868) - 6.4836 \times 10^{-9}(T - 249.868)^2$$

$$\left[\frac{\text{V}}{\text{N} \cdot \text{m}} \right]$$

This varies with torque but the first term is very similar to the linear best fit result. The 3rd order polynomial fit produced a correlation with $R^2 = 0.999$, an error of

0.065 % FS and a measurement error of ± 0.325 N.m. These results are certainly better than the linear best fit but in many applications the linear best fit should suffice.

Figure 11 shows the hysteresis of the sensor as it cycles from zero to 500 N.m and back. The solid lines are polynomial fit curves to the raw data. The maximum horizontal displacement of the two curves is approximately 8 N.m representing an error of 0.016 %.

5 Conclusions

A general method of torque sensing in machine shafts and similar structures has been presented. The method is noncontact and accurate and applicable to static and dynamic measurement of torque. The use of a magnetoelastic sleeve allows consistent sensing and the eddy current probes used allow use of commonly available eddy current instruments, simplifying design. The results presented show accuracies of the order of 0.1 % FS with very low hysteresis. The final probe configuration was designed to keep a constant gap between its tips and the magnetoelastic sleeve. The transfer function, although not perfectly linear is very close and a linear fit may be used to represent the output. Alternatively, a 3rd order polynomial fit can be used with improved accuracy.

References

1. Zabler, E., Heintz, F., Dukart, A., & Krott, P. *A non contact strain gage torque sensor for automotive servo driven steering systems*. SAE Paper 940629. Copyright Society of Automotive Engineers, Inc.
2. Fleming, W. J. (1990). *Magnetostrictive torque sensors—comparison of branch, cross, and solenoidal designs*. SAE Paper 900264. Detroit, MI: International Congress and Exposition.
3. Lemarquand, V., & Lemarquand, G. (1995). Magnetic differential torque sensor. *IEEE Transactions on Magnetics*, 31(6), 3188–3190.
4. U.S. Patent No. 5,841,132, Horton, S. J., Trace, A. L., & Rees, D. (1998) *Optical displacement sensor and torque sensor employing relatively movable slit patterns*.
5. U.S. Patent No. 4,907,460, Taniguchi, M., Nagano, H., Daido, T., Kuramoto, I., Nohara, M., & Kyotani, H. (1990). *Torque sensor*.
6. Son, D., Lim, S. J., & Kim, C. S. (1992). Non-contact torque sensor using the difference of maximum induction of amorphous cores. *IEEE Transactions on Magnetics*, 28(5), 2205–2207.
7. European Patent # DE 3437379 A1, Bently Nevada Corp (1984). *Arrangement for measuring of the torsion force or bending force applied to a shaft*.
8. Carpenter Steel Division, *Soft magnetic alloys*. Alloy Data Catalog by Carpenter Technology Co., Reading, PA 19612-4662.